Delay-based Decoupling of Power System Models for Transient Stability Analysis

Georgios Tzounas, *Student Member, IEEE*, Federico Milano, *Fellow, IEEE*

***Abstract*— This paper proposes a delay-based method to reduce the coupling of the equations of power system models for transient stability analysis. The method consists in identifying the variables that, when subjected to a delay equal to the time step of the numerical integration (one-step delay), leave practically unchanged the system trajectories. Automatic selection of the variables based on a geometric controllability/observability approach and estimation of the maximum admissible delay are duly discussed. Such a one-step-delay approximation increases the sparsity of the system Jacobian matrices and can be used in conjunction with state-of-the-art techniques for the integration of differential-algebraic equations. The proposed approach is evaluated in terms of accuracy, convergence and computational burden, by means of the New England 39-bus system; a 21,177-bus model of the ENTSO-E transmission system.**

***Index Terms*— Time Domain Integration (TDI), Delay Differential Algebraic Equations (DDAEs), Small Signal Stability Analysis (SSSA), geometric approach.**

I. INTRODUCTION

A. Motivation

The power system model for rotor-angle and voltage stability analysis is traditionally formulated as a set of Differential Algebraic Equations (DAEs). These equations are mutually dependent due to the meshed topology of transmission networks and the action of secondary controllers. This paper focuses on the inclusion of fictitious time delays that, while not altering the overall dynamic response of the system, allows reducing the coupling of the DAEs by removing off-diagonal elements of the system Jacobian matrix.

B. Literature Review

Introducing time delays in a set of DAEs turns it into a set of Functional DAEs (FDAEs), namely FDAEs of retarded type, also known as Delay Differential Algebraic Equations (DDAEs). DDAEs are typically employed to model physical time delays. These are inherent to many engineering applications, such as circuit and microwave theory [1], [2]. In power systems, delays have been considered to study the effect of long transmission lines [3] and, more recently, the latency of communication networks, which affects wide area measurement systems and controllers [4], [5]. Other studies consider delays arising in the coordination of electric vehicles that participate in load frequency control [6] and in phase-locked loops for frequency estimation [7].

A property of constant delays is that the Jacobian elements with respect to retarded variables are null. This feature has been utilized for the simulation of Electro-Magnetic Transients (EMTs) that include long transmission lines [8] or control systems [9]. The sending- and receiving-end variables of long overhead lines, in fact, are decoupled by the transmission delay and, hence, sections of circuits connected through long lines are naturally decoupled. In [9], on the other hand, the control system is solved at the previous step of the EMT circuit equations which, *de facto*, introduced a delay in the control equations. This allows ordering the Jacobian matrix of the DAEs with a block diagonal structure (see Fig. 1.a). Each block can be handled separately at each time step – which is of the same order of the delay, i.e. μs – and allows exploiting parallelization techniques.

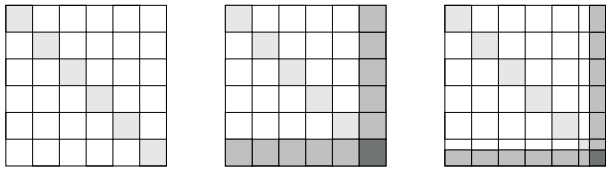

(a) (b) (c)

Fig. 1: Types of Jacobian matrices: (a) block-diagonal matrix of a fully decoupled system; (b) coupled system ordered to exploit the BBD structure; and (c) coupled system with ordered BBD structure and extra decoupling obtained through fictitious delays.

The effort of developing parallel algorithms in EMT simulations stems from the fact that simulations of this type are slow for large systems [10]. For systems with the same number of buses, simulations based on quasi-steady state phasors and electromechanical models are much faster. However, the Time Domain Integration (TDI) of large power systems requires iteratively solving stiff nonlinear hybrid DAEs, which is still a time-consuming task to complete. The time required to complete a $N-1$ contingency analysis, in fact, can be a critical constraint, e.g. for on-line dynamic security assessment (see, for example, Chapter 15 of [11]).

The DAEs for transient stability analysis are naturally coupled through the admittance matrix of the grid, which is modeled with a set of algebraic equations, as well as by secondary frequency controllers, and generally do not include delays. This leads to a Bordered Block Diagonal (BBD) structure of the Jacobian matrix (see Fig. 1.b) [12]. The BBD structure can be enforced in any set of DAEs through *diakoptics*, i.e. by introducing additional algebraic equations [13], [14]. Such equations increase the order of the system but tend to increase sparsity and, in some cases, may also speed up the factorization of the Jacobian matrix of the system. A technique conceptually similar to diakoptics, called MANA, namely Modified Augmented Nodal Analysis,

has been utilized in unbalanced power flow analysis [15] and EMTs [16] but has no clear application for single-phase equivalent phasor-based transient stability models.

The main idea of this paper is that, if one includes fictitious delays in the power system transient stability model, the Jacobian matrix can be further decoupled (see Fig. 1.c) without increasing the system's order, thus increasing sparsity and reducing the computational burden of numerical methods. In this vein, in [17], the authors proposed the use of the Center of Inertia (COI) at the previous time step to decouple the equations of the rotor angles of the synchronous machines. In [17], the "slightly" delayed COI was tested on a 4-bus system using the Implicit Trapezoidal Method (ITM) with time step 0.01 s and showed not to affect the system transient response.

To the best of our knowledge, there is no study that proposes a systematic way to implement and evaluate the one-step delay approximation for a DAE model for transient stability analysis. This paper attempts to fill this gap by recognizing that the one-step-delay approximation in a coupled system can be formally studied as a set of DDAEs.

C. Contributions

The contributions of this paper are as follows:

- A rigorous and systematic analysis of the impact of the one-step delay approximation on the accuracy, convergence and computational burden of the time domain integration routine.
- A method to identify the elements of a power system DAE model that can be delayed by one time step, as well as a technique to estimate the maximum admissible delay, so that the approximation is within a given tolerance. This analysis has to be carried out only once per network.

D. Organization

The remainder of the paper is organized as follows. Section II recalls a conventional implicit TDI scheme for power systems. Section III discusses the proposed approach to one-step-delay approximation. Section IV discusses how to select the variables of a DAE model to be delayed. Section V provides a method to calculate the maximum admissible delay for a given DDAE model. The case study is discussed in Section VI. Conclusions are drawn and future work is outlined in Section VII.

II. Implicit Integration of Power System

Power systems are conventionally modeled as a set of explicit non-linear DAEs, as follows:

$$\begin{aligned} \dot{\boldsymbol{x}} &= \boldsymbol{f}(\boldsymbol{x}, \boldsymbol{y}) \\ \mathbf{0} &= \boldsymbol{g}(\boldsymbol{x}, \boldsymbol{y}) \ , \end{aligned} \tag{1}$$

where $\boldsymbol{f}$ ($\boldsymbol{f} : \mathbb{R}^{(n+m)} \rightarrow \mathbb{R}^n$), $\boldsymbol{g}$ ($\boldsymbol{g} : \mathbb{R}^{(n+m)} \rightarrow \mathbb{R}^m$), are the differential, algebraic equations, respectively; $\boldsymbol{x} = \boldsymbol{x}(t)$, $\boldsymbol{x} \in \mathbb{R}^n$, are the state variables, $\boldsymbol{y} = \boldsymbol{y}(t)$, $\boldsymbol{y} \in \mathbb{R}^m$, are the algebraic variables; and $t \in [0, +\infty)$ is the simulation time.

In this formulation, discrete variables are modeled implicitly, i.e. each discontinuous change in the system leads to a new continuous set of equations in the form of (1). Equations (1) are stiff, for two reasons: (i) the time constants of the differential equations typically span multiple time scales; and (ii) the algebraic equations can be viewed as *infinitely fast* differential equations associated with zero time constants.

Explicit numerical methods are known to perform poorly for stiff problems. Thus, a common approach to numerically integrate (1) is to use an implicit method with a direct solver. Employing an implicit method allows a simultaneous solution of both state and algebraic variables [18], and requires the solution of the following set of nonlinear equations:

$$\begin{aligned} \mathbf{0} &= \boldsymbol{r}(\boldsymbol{x}, \boldsymbol{y}, h) \\ \mathbf{0} &= \boldsymbol{s}(\boldsymbol{x}, \boldsymbol{y}, h) \ , \end{aligned} \tag{2}$$

where $\boldsymbol{r}$, ($\boldsymbol{r} : \mathbb{R}^{(n+m)} \rightarrow \mathbb{R}^n$) and $\boldsymbol{s}$, ($\boldsymbol{s} : \mathbb{R}^{(n+m)} \rightarrow \mathbb{R}^m$) are nonlinear functions that depend on the differential and algebraic equations, respectively, as well as on the applied implicit method. The update of the state and algebraic variables at each time step can be expressed as follows:

$$\begin{bmatrix} \boldsymbol{x}^{(i+1)}(t+h) \\ \boldsymbol{y}^{(i+1)}(t+h) \end{bmatrix} = \begin{bmatrix} \boldsymbol{x}^{(i)}(t+h) \\ \boldsymbol{y}^{(i)}(t+h) \end{bmatrix} + \begin{bmatrix} \Delta\boldsymbol{x}^{(i)} \\ \Delta\boldsymbol{y}^{(i)} \end{bmatrix} \ , \tag{3}$$

where h is the time step length; $\boldsymbol{x}^{(i)}(t+h)$ denotes the vector $\boldsymbol{x}$ at the i-th iteration of time $t+h$. The increments $\Delta\boldsymbol{x}^{(i)}$, $\Delta\boldsymbol{y}^{(i)}$ are obtained by employing the Newton method, as follows:

$$\begin{bmatrix} \Delta\boldsymbol{x}^{(i)} \\ \Delta\boldsymbol{y}^{(i)} \end{bmatrix} = -\left[\boldsymbol{A}_c^{(i)}\right]^{-1} \begin{bmatrix} \boldsymbol{r}^{(i)} \\ \boldsymbol{s}^{(i)} \end{bmatrix} \ , \tag{4}$$

where $\boldsymbol{A}_c^{(i)}$, $\boldsymbol{A}_c^{(i)} \in \mathbb{R}^{(n+m)\times(n+m)}$, is defined as:

$$\boldsymbol{A}_c^{(i)} = \begin{bmatrix} \boldsymbol{r}_{\boldsymbol{x}}^{(i)} & \boldsymbol{r}_{\boldsymbol{y}}^{(i)} \\ \boldsymbol{s}_{\boldsymbol{x}}^{(i)} & \boldsymbol{s}_{\boldsymbol{y}}^{(i)} \end{bmatrix} \ , \tag{5}$$

where $\boldsymbol{r}_{\boldsymbol{x}}^{(i)}$, $\boldsymbol{r}_{\boldsymbol{y}}^{(i)}$, $\boldsymbol{s}_{\boldsymbol{x}}^{(i)}$, $\boldsymbol{s}_{\boldsymbol{y}}^{(i)}$ are the Jacobian matrices of $\boldsymbol{r}$ and $\boldsymbol{s}$ at the i-th iteration of time t.

Among the various implicit numerical methods utilized by power system software tools to define equations (2), for simplicity but without lack of generality, we consider only one, namely the ITM. The discussion below can be easily applied to any other method. The ITM leads to the following form of (2):

$$\begin{aligned} \mathbf{0} &= \boldsymbol{r}^{(i)} = \boldsymbol{x}^{(i)} - \boldsymbol{x}(t-h) - 0.5h\big(\boldsymbol{f}^{(i)} + \boldsymbol{f}(t-h)\big) \\ \mathbf{0} &= \boldsymbol{s}^{(i)} = \boldsymbol{g}^{(i)} \ , \end{aligned} \tag{6}$$

where h is the time step length; $\boldsymbol{f}^{(i)} = \boldsymbol{f}(\boldsymbol{x}^{(i)}, \boldsymbol{y}^{(i)})$, $\boldsymbol{g}^{(i)} = \boldsymbol{g}(\boldsymbol{x}^{(i)}, \boldsymbol{y}^{(i)})$ and $\boldsymbol{f}(t-h) = \boldsymbol{f}(\boldsymbol{x}(t-h), \boldsymbol{y}(t-h))$. The Jacobian matrix (5) at the i-th iteration of time t is defined as:

$$\begin{aligned} \boldsymbol{r}_{\boldsymbol{x}}^{(i)} &= \boldsymbol{I}_n - 0.5h\boldsymbol{f}_{\boldsymbol{x}}^{(i)} \ , \ \boldsymbol{r}_{\boldsymbol{y}}^{(i)} = -0.5h\boldsymbol{f}_{\boldsymbol{y}}^{(i)} \ , \\ \boldsymbol{s}_{\boldsymbol{x}}^{(i)} &= \boldsymbol{g}_{\boldsymbol{x}}^{(i)} \ , \ \boldsymbol{s}_{\boldsymbol{y}}^{(i)} = \boldsymbol{g}_{\boldsymbol{y}}^{(i)} \ , \end{aligned} \tag{7}$$

where $\boldsymbol{f}_{\boldsymbol{x}}^{(i)}$, $\boldsymbol{f}_{\boldsymbol{y}}^{(i)}$, $\boldsymbol{g}_{\boldsymbol{x}}^{(i)}$, $\boldsymbol{g}_{\boldsymbol{y}}^{(i)}$ are the Jacobian matrices of the DAEs; and $\boldsymbol{I}_n$ denotes the identity matrix of order n.

III. One-Step-Delay Approximation

Let us assume that some variables – we will discuss later how to select such variables – of the DAE system (1) are substituted with their values at the previous time step. Such a system can be formally studied as a system of nonlinear DDAEs with inclusion of a constant delay, as follows:

$$\begin{aligned} \dot{\boldsymbol{x}} &= \tilde{\boldsymbol{f}}(\boldsymbol{x}, \boldsymbol{y}, \boldsymbol{x}_d, \boldsymbol{y}_d) \\ \boldsymbol{0} &= \tilde{\boldsymbol{g}}(\boldsymbol{x}, \boldsymbol{y}, \boldsymbol{x}_d, \boldsymbol{y}_d) \ , \end{aligned} \tag{8}$$

where $\boldsymbol{x}_d$, $\boldsymbol{x}_d \in \mathbb{R}^{n_d}$, $\boldsymbol{y}_d$, $\boldsymbol{y}_d \in \mathbb{R}^{m_d}$, are the delayed state and algebraic variables, respectively, as follows:

$$\boldsymbol{x}_d = \boldsymbol{x}(t-h) \ , \ \boldsymbol{y}_d = \boldsymbol{y}(t-h) \ . \tag{9}$$

Note that (8) is an approximation of (1). The delay h, in fact, is fictitious as it does not model any physical phenomenon.

The numerical integration of (8) requires the solution of the following set of nonlinear equations [19]:

$$\begin{aligned} \boldsymbol{0} &= \tilde{\boldsymbol{r}}(\boldsymbol{x}, \boldsymbol{y}, \boldsymbol{x}_d, \boldsymbol{y}_d, h) \\ \boldsymbol{0} &= \tilde{\boldsymbol{s}}(\boldsymbol{x}, \boldsymbol{y}, \boldsymbol{x}_d, \boldsymbol{y}_d, h) \ . \end{aligned} \tag{10}$$

If at the i-th iteration of time t, $\tilde{\boldsymbol{f}}_{\boldsymbol{x}}^{(i)}$, $\tilde{\boldsymbol{f}}_{\boldsymbol{y}}^{(i)}$, $\tilde{\boldsymbol{g}}_{\boldsymbol{x}}^{(i)}$, $\tilde{\boldsymbol{g}}_{\boldsymbol{y}}^{(i)}$, are the delay-free and $\tilde{\boldsymbol{f}}_{\boldsymbol{x}_d}^{(i)}$, $\tilde{\boldsymbol{f}}_{\boldsymbol{y}_d}^{(i)}$, $\tilde{\boldsymbol{g}}_{\boldsymbol{x}_d}^{(i)}$, $\tilde{\boldsymbol{g}}_{\boldsymbol{y}_d}^{(i)}$, are the Jacobian matrices of the delayed variables of system (8), then the following identities apply:

$$\begin{aligned} \boldsymbol{f}_{\boldsymbol{x}}^{(i)} &= \tilde{\boldsymbol{f}}_{\boldsymbol{x}}^{(i)} + \tilde{\boldsymbol{f}}_{\boldsymbol{x}_d}^{(i)} \ , \ \boldsymbol{f}_{\boldsymbol{y}}^{(i)} = \tilde{\boldsymbol{f}}_{\boldsymbol{y}}^{(i)} + \tilde{\boldsymbol{f}}_{\boldsymbol{y}_d}^{(i)} \ , \\ \boldsymbol{g}_{\boldsymbol{x}}^{(i)} &= \tilde{\boldsymbol{g}}_{\boldsymbol{x}}^{(i)} + \tilde{\boldsymbol{g}}_{\boldsymbol{x}_d}^{(i)} \ , \ \boldsymbol{g}_{\boldsymbol{y}}^{(i)} = \tilde{\boldsymbol{g}}_{\boldsymbol{y}}^{(i)} + \tilde{\boldsymbol{g}}_{\boldsymbol{y}_d}^{(i)} \ . \end{aligned} \tag{11}$$

The main difference between (10) and (2) is that the Jacobian matrices of (10) do not include the terms that depend on $\boldsymbol{x}_d$ and $\boldsymbol{y}_d$, as these variables are "constants" at time t. We have:

$$\begin{bmatrix} \Delta \boldsymbol{x}^{(i)} \\ \Delta \boldsymbol{y}^{(i)} \end{bmatrix} = - \left[\tilde{\boldsymbol{A}}_c^{(i)} \right]^{-1} \begin{bmatrix} \tilde{\boldsymbol{r}}^{(i)} \\ \tilde{\boldsymbol{s}}^{(i)} \end{bmatrix} \ , \tag{12}$$

where

$$\tilde{\boldsymbol{A}}_c^{(i)} = \begin{bmatrix} \tilde{\boldsymbol{r}}_{\boldsymbol{x}}^{(i)} & \tilde{\boldsymbol{r}}_{\boldsymbol{y}}^{(i)} \\ \tilde{\boldsymbol{s}}_{\boldsymbol{x}}^{(i)} & \tilde{\boldsymbol{s}}_{\boldsymbol{y}}^{(i)} \end{bmatrix} \ . \tag{13}$$

The terms $\tilde{\boldsymbol{r}}_{\boldsymbol{x}}^{(i)}$, $\tilde{\boldsymbol{r}}_{\boldsymbol{y}}^{(i)}$, $\tilde{\boldsymbol{s}}_{\boldsymbol{x}}^{(i)}$, $\tilde{\boldsymbol{s}}_{\boldsymbol{y}}^{(i)}$ are the delay-free Jacobian matrices of $\tilde{\boldsymbol{r}}^{(i)}$ and $\tilde{\boldsymbol{s}}^{(i)}$. For a detailed description on the modifications required by the ITM in order to integrate a set of DDAEs with inclusion of more general (time-varying and state-dependent) delays, the interested reader may refer to [19]. Since matrix $\tilde{\boldsymbol{A}}_c$ is composed only of the delay-free Jacobian matrix elements of $\tilde{\boldsymbol{r}}$ and $\tilde{\boldsymbol{s}}$, $\tilde{\boldsymbol{A}}_c$ is sparser than $\boldsymbol{A}_c$. The scope of this paper is to take advantage of the fact that approximating (1) with (8) leads to a sparser Jacobian matrix.

IV. Selection of Variables to be Delayed

Inclusion of fictitious time delays in a set of DAEs introduces an inevitable approximation in its transient response. It is thus crucial to identify the variables and the equations that, if subject to a small variation, do not lead to a significant change in the system trajectories. With this regard, delaying variables that are slower than the dynamics of main interest, causes a smaller variation in the system trajectories.

Another aspect is the position of the selected elements in the Jacobian matrix. Removing elements that introduce dense rows/columns in the Jacobian leads not only to a sparsity increase, but also to decoupling of the system equations, which in turn allows exploiting state-of-the-art algorithms that parallelize the factorization. Such algorithms usually exploit the specific formulation of current-injection power system models and the admittance matrix to take advantage of the BBD structure of the Jacobian matrix [20], [21]. Exploiting parallelization, however, is out of the scope of this paper. Thus we have adopted the general DAE model described by (1).

A. Systematic Selection of Variables

In this section, we provide a systematic small signal based method to select the delayed variables $\boldsymbol{x}_d$ and $\boldsymbol{y}_d$ of a model, based on the geometric approach discussed in [22]. The geometric approach has been widely employed in control design to provide a measure for (i) the observability of a dynamic mode from a signal; (ii) the controllability of a mode from a control input placement. Combining the two provides the joint controllability/observability index. The smaller this index is, the less the examined mode is affected by the specific signal-control input set. In the following, we utilize the geometric approach to determine the sensitivity of system modes to variations of all non-zero elements of the DAE Jacobian matrices. Differentiating (1) around an equilibrium point yields:

$$\begin{aligned} \Delta \dot{\boldsymbol{x}} &= \boldsymbol{f}_{\boldsymbol{x}} \Delta \boldsymbol{x} + \boldsymbol{f}_{\boldsymbol{y}} \Delta \boldsymbol{y} \\ \boldsymbol{0} &= \boldsymbol{g}_{\boldsymbol{x}} \Delta \boldsymbol{x} + \boldsymbol{g}_{\boldsymbol{y}} \Delta \boldsymbol{y} \ . \end{aligned} \tag{14}$$

Elimination of $\Delta \boldsymbol{y}$ leads to $\Delta \dot{\boldsymbol{x}} = \boldsymbol{A} \Delta \boldsymbol{x}$, where the matrix $\boldsymbol{A} = \boldsymbol{f}_{\boldsymbol{x}} - \boldsymbol{f}_{\boldsymbol{y}} \boldsymbol{g}_{\boldsymbol{y}}^{-1} \boldsymbol{g}_{\boldsymbol{x}}$ has n finite eigenvalues $\lambda_1, \lambda_2, \ldots, \lambda_n$. Complex conjugate eigenvalues, say $\lambda_i = \sigma_i \pm j w_i$, define oscillatory modes with natural frequency $f_i = w_i / 2\pi$. For rotor angle stability studies, modes of interest are those with $f_i \in [0.1, 2]$ Hz [23]. In the remainder of the paper, we refer to such modes (and the respective eigenvalues) as *relevant*.

Let us now introduce a perturbation into (14), as follows:

$$\begin{aligned} \Delta \dot{\boldsymbol{x}} &= \boldsymbol{f}_{\boldsymbol{x}} \Delta \boldsymbol{x} + \boldsymbol{f}_{\boldsymbol{y}} \Delta \boldsymbol{y} + \boldsymbol{B}_f \Delta \boldsymbol{u}_f \\ \boldsymbol{0} &= \boldsymbol{g}_{\boldsymbol{x}} \Delta \boldsymbol{x} + \boldsymbol{g}_{\boldsymbol{y}} \Delta \boldsymbol{y} + \boldsymbol{B}_g \Delta \boldsymbol{u}_g \ , \end{aligned} \tag{15}$$

where $\Delta \boldsymbol{u}_f \in \mathbb{R}^n$, $\Delta \boldsymbol{u}_g \in \mathbb{R}^m$ are the perturbation vectors of the differential, algebraic equations, respectively; and $\boldsymbol{B}_f$, $\boldsymbol{B}_g$ are the perturbation matrices associated with $\Delta \boldsymbol{u}_f$ and $\Delta \boldsymbol{u}_g$, respectively. Eliminating $\Delta \boldsymbol{y}$ from (15) yields:

$$\Delta \dot{\boldsymbol{x}} = \boldsymbol{A} \Delta \boldsymbol{x} + \boldsymbol{B}_f \Delta \boldsymbol{u}_f - \boldsymbol{f}_{\boldsymbol{y}} \boldsymbol{g}_{\boldsymbol{y}}^{-1} \boldsymbol{B}_g \Delta \boldsymbol{u}_g \ . \tag{16}$$

Considering zero perturbation matrices in (16), as discussed in [22], we can define the output matrices of the state and algebraic variable variations as $\boldsymbol{C}_x = \boldsymbol{I}_n$, $\boldsymbol{C}_y = -\boldsymbol{g}_{\boldsymbol{y}}^{-1} \boldsymbol{g}_{\boldsymbol{x}}$, respectively. Let also $\boldsymbol{J} = \{\boldsymbol{f}, \boldsymbol{g}\}$ and $\boldsymbol{z} = \{\boldsymbol{x}, \boldsymbol{y}\}$, so that $\boldsymbol{J}_{\boldsymbol{z}}$ is a compact notation for any of the Jacobians $\boldsymbol{f}_{\boldsymbol{x}}$, $\boldsymbol{f}_{\boldsymbol{y}}$, $\boldsymbol{g}_{\boldsymbol{x}}$ and $\boldsymbol{g}_{\boldsymbol{y}}$. With $\boldsymbol{J}_{\boldsymbol{z}}(\mu_J, \nu_z)$ we denote the μ_J-th row, ν_z-th column element of $\boldsymbol{J}_{\boldsymbol{z}}$. Finally, let $\boldsymbol{\phi}_i$ and $\boldsymbol{\psi}_i$ be the right and left eigenvectors associated with the relevant eigenvalue λ_i, respectively. That said, the geometric

controllability/observability measures of λ_i from the Jacobian matrix elements of the system are determined as follows:

$$\mathrm{gco}(\boldsymbol{J_z}(\mu_J,\nu_z)) = \frac{|\boldsymbol{c}_{z,\mu_J}\boldsymbol{\phi}_i\boldsymbol{\psi}_i\boldsymbol{b}_{J,\nu_z}|}{||\boldsymbol{\phi}_k||\ ||\boldsymbol{c}_{z,\mu_J}||\ ||\boldsymbol{\psi}_i||\ ||\boldsymbol{b}_{J,\nu_z}||}\ , \quad (17)$$

where $\boldsymbol{c}_{z,\mu_J}$ is the μ_J-th row of the output matrix $\boldsymbol{C}_z$; $\boldsymbol{b}_{J,\nu_z}$ is the ν_z-th column of the perturbation matrix $\boldsymbol{B}_J$; $|\cdot|$ and $||\cdot||$ denote the modulus and Euclidean norm, respectively.

Expression (17) allows selecting the elements of the Jacobians of (14) that can be delayed and thus can be eliminated from the matrices $\boldsymbol{f_x}$, $\boldsymbol{f_y}$, $\boldsymbol{g_x}$ and $\boldsymbol{g_y}$. Specifically, elements of such matrices that have low gco values for all relevant modes of the system, do not noticeably impact the dynamic behavior of the system. Therefore, we select as a candidate to be delayed any element whose gco value is below a given threshold $\mathrm{gco}_{\max}$. Note that $\boldsymbol{f_x}$, $\boldsymbol{f_y}$, $\boldsymbol{g_x}$ and $\boldsymbol{g_y}$ are stored as sparse matrices, hence only non-zero elements are considered for the analysis above, which leads to an efficient implementation.

B. Illustrative Examples

The criteria described above are further discussed through some illustrative examples, which are based on well-known devices and models utilized in transient stability analysis. In particular, we consider devices and controllers that are slow and/or couple several variables of the systems.

Center-of-Inertia: The algebraic variable of the COI speed (ω_{COI}) is defined by the following algebraic equation:

$$g_{(\omega_{\mathrm{COI}})} := 0 = \omega_{\mathrm{COI}} - \sum_{i=1}^{\kappa}\frac{M_i}{M_T}\omega_i\ , \quad (18)$$

where ω_i, $i = 1,2,\ldots,\kappa$, is the state of the speed of the i-th machine; M_i is the mechanical starting time of the i-th machine; and $M_T = M_1 + M_2 + \ldots + M_\kappa$. The COI speed is used as a reference in the differential equations of the generator rotor angles:

$$f_{(\dot{\delta}_i)} := \dot{\delta}_i = \Omega_b\big(\omega_i - \omega_{\mathrm{COI}}\big)\ , \quad (19)$$

where Ω_b is the angular frequency base. The COI provides the "average" frequency trend of the system and thus represents a relatively slow dynamic. Delaying the ω_i's and ω_{COI} in (18), (19), respectively, allows removing the elements $\partial g_{(\omega_{\mathrm{COI}})}/\partial\omega_i$ and $\partial f_{(\dot{\delta}_i)}/\partial\omega_{\mathrm{COI}}$, which constitute a dense row in $\boldsymbol{g_x}$ and a dense column in $\boldsymbol{f_y}$, respectively.

Turbine Governor: The action of some Turbine Governors (TGs) can be significantly slow, as compared to primary damping and voltage controllers and hence, adding one-step delays in some TG DAE models, e.g. the ones described in [24], leads to increased sparsity without jeopardizing the TDI accuracy. On the other hand, since TG variables typically do not constitute dense segments in the Jacobian matrix, the increased sparsity does not come with significant decoupling.

Automatic Generation Control: Automatic Generation Control (AGC) is used to provide secondary frequency regulation to the power system. Consider a simplified continuous AGC model that measures the COI frequency and produces a dynamic active power command (p_{s}) which is distributed to the machine TGs proportionally to their droops [25]. The algebraic variable of the power order received by the i-th TG is defined by the following algebraic equation:

$$g_{(p_{\mathrm{ord},i})} := 0 = p_{\mathrm{ord},i} - \frac{R_i}{R_T}p_{\mathrm{s}}\ , \quad (20)$$

where $p_{\mathrm{ord},i}$ is the TG power order; R_i is the droop constant; and $R_T = R_1 + R_2 + \ldots + R_\kappa$. Delaying $p_{\mathrm{ord},i}$ in (20) removes $\partial g_{(p_{\mathrm{ord},i})}/\partial p_{\mathrm{s}}$, which forms a dense column in $\boldsymbol{g_x}$, while accuracy is not impacted, because of the AGC slow action.

Secondary Voltage Regulation: The Secondary Voltage Regulation (SVR) model employed in this paper is based on the scheme proposed in the grid code of the Italian system. For a detailed description of this scheme, the interested reader may refer to [26]. The SVR mainly consists of two control levels. The external loop receives the voltage measurement of a selected pilot bus and computes the vector $\boldsymbol{q}_{\mathrm{ref}}$ that represents reactive power limits for the participating to the SVR generators. $\boldsymbol{q}_{\mathrm{ref}}$ is compared with the actual reactive power generation vector $\boldsymbol{q}$ and the error $\boldsymbol{q}_{\mathrm{r}} = \boldsymbol{q}_{\mathrm{ref}} - \boldsymbol{q}$ is further processed by a dynamic decoupling matrix $\boldsymbol{D}$. The produced vector is finally sent to the Generator Reactive Power Regulators (GRPRs). Each GRPR is basically a PI control, the output of which is considered as input to the voltage reference of the generator's Automatic Voltage Regulation (AVR). The dynamic behavior of the the i-th GRPR state variable $x_{r,i}$ is given by the PI differential equation:

$$f_{(x_{r,i})} := \dot{x}_{r,i} = K_I\boldsymbol{D}_i\boldsymbol{q}_{\mathrm{r}}\ , \quad (21)$$

where K_I is the integral gain of the GRPR; $\boldsymbol{D}_i$ is the i-th row of $\boldsymbol{D}$. Delaying $\boldsymbol{q}_{\mathrm{r}}$ in (21) allows eliminating $\partial f_{(x_{r,i})}/\partial\boldsymbol{q}_{\mathrm{r}}$, which constitutes a dense block of columns and rows in $\boldsymbol{f_y}$. The accuracy of the integration is maintained, due to the relatively slow time scale of the SVR action.

V. Maximum Delay / Time Step

We provide a technique based on SSSA (Small Signal Stability Analysis), which for a selected set of $\boldsymbol{x}_d$ and $\boldsymbol{y}_d$, estimates the maximum admissible delay $h_{\max}$ that allows keeping the errors between the original DAEs and the modified DDAEs below a threshold. To this aim, we first solve the eigenvalue problem of the linearized delayed system. Linearizing (8) around a valid operating point yields:

$$\begin{aligned}\Delta\dot{\boldsymbol{x}} &= \tilde{\boldsymbol{f}}_{\boldsymbol{x}}\Delta\boldsymbol{x} + \tilde{\boldsymbol{f}}_{\boldsymbol{y}}\Delta\boldsymbol{y} + \tilde{\boldsymbol{f}}_{\boldsymbol{x}_d}\Delta\boldsymbol{x}_d + \tilde{\boldsymbol{f}}_{\boldsymbol{y}_d}\Delta\boldsymbol{y}_d\\ \boldsymbol{0} &= \tilde{\boldsymbol{g}}_{\boldsymbol{x}}\Delta\boldsymbol{x} + \tilde{\boldsymbol{g}}_{\boldsymbol{y}}\Delta\boldsymbol{y} + \tilde{\boldsymbol{g}}_{\boldsymbol{x}_d}\Delta\boldsymbol{x}_d + \tilde{\boldsymbol{g}}_{\boldsymbol{y}_d}\Delta\boldsymbol{y}_d\ .\end{aligned} \quad (22)$$

Eliminating the algebraic variables from (22) is possible under the assumption that $\tilde{\boldsymbol{g}}_y$ is not singular, as follows:

$$\Delta\dot{\boldsymbol{x}} = \boldsymbol{A}_0\Delta\boldsymbol{x} + \boldsymbol{A}_1\Delta\boldsymbol{x}_d + \sum_{k=2}^{\infty}(\boldsymbol{A}_k\boldsymbol{x}(t-kh))\ , \quad (23)$$

where $\boldsymbol{A}_0$ is the delay-free system matrix; $\boldsymbol{A}_k$, $k \geq 2$, are the delayed system matrices. A rigorous proof of (23), as well as the condition under which the series in (23) converges, are provided in [27]. The series typically converges rapidly as k increases and, thus, it is acceptable to assume a finite maximum value for k, say ρ, in the summation of (23), and

hence, the characteristic matrix of (23) can be approximated with the following pencil:

$$s\,\boldsymbol{I}_n - \boldsymbol{A}_0 - \sum_{k=1}^{\rho}(e^{-skh}\boldsymbol{A}_k)\ . \tag{24}$$

We are now ready to provide the following proposition on the continuity of the eigenvalues of (24).

Proposition 1.

Let $\hat{\lambda}$ be an eigenvalue of (24) with multiplicity α. There exists a constant $\hat{\epsilon}$ such that for all $\epsilon > 0$ satisfying $\epsilon < \hat{\epsilon}$, there is a number $\xi > 0$ such that the pencil:

$$s\,\boldsymbol{I}_n - (1+\xi)\left[\boldsymbol{A}_0 - \sum_{k=1}^{\rho} e^{-sk(1+\xi)h}\boldsymbol{A}_k\right]\ , \tag{25}$$

where

$$\begin{aligned}&\xi h \in \mathbb{R}, \qquad ||\xi h|| < \xi,\ h + \xi h \geq 0,\\ &\xi \boldsymbol{A}_k \in \mathbb{R}^{n\times n},\ ||\xi \boldsymbol{A}_k||_2 < \xi,\ k = 0, 1, \ldots, \rho,\end{aligned}$$

has exactly α eigenvalues in the disk: $\{s \in \mathbb{C} : |s - \hat{\lambda}| < \epsilon\}$. The notation $||\cdot||_2$ implies the induced matrix 2-norm.

The proposition above states that the characteristic roots of a delayed system behave continuously with respect to variations of system matrices and delays [28].

In the proposed scheme, the modes of the time delay system are viewed as approximations of the modes of the delay-free system. Let λ_i and $\hat{\lambda}_i$ be the i-th rightmost, non-null eigenvalues of the delay-free and the delayed system, respectively. The associated relative error is:

$$\eta_i = \frac{|\hat{\lambda}_i - \lambda_i|}{|\lambda_i|}\ . \tag{26}$$

The limit case $h = 0$ leads to $\eta_i = 0,\ \ 0 \leq i \leq n$; and, for $h > 0$, $\eta_i \geq 0$. Assigning a maximum admissible error, say $\eta_{\max}$, allows finding the delay upper bound $h_{\max}$, as follows:

$$\eta_{\max} \geq \frac{|\hat{\lambda}_i(h_{\max}) - \lambda_i|}{|\lambda_i|}, \quad \forall i = 1, 2, \ldots, \nu,\ \nu \leq n\ . \tag{27}$$

The calculation of $h_{\max}$ requires to find the eigenvalues of (24), which implies solving a non-linear, transcendental characteristic equation. Transforming (24) into a linear pencil is possible by using a partial differential equations representation of the system, which however, has infinite dimensions. A reduced set of eigenvalues can be found by employing a Chebyshev discretization scheme, which has been successfully applied to power systems with inclusion of time-delays [19].

The following remarks are relevant.

1) Delay vs time step: In general, the time step of the numerical integration is determined based on the fastest dynamics of the system, whereas the variables that are delayed in this work are typically associated with slow dynamics. This means that the time step is always smaller than the time scale of delayed variables. Regarding the magnitude of the time delay, if the delay is greater than the integration time step, an extra, undesirable approximation is introduced into the system, as Proposition 1 indicates that the difference between the DAEs and DDAEs are the smaller, the smaller is the delay. On the other hand, for delays smaller than the time step, the numerical integration has to interpolate the delayed values, which introduces an additional source of error in the trajectories of the DDAEs. In general, handling delays smaller than the step size is an open research topic, as it creates difficulties even for special integration methods for stiff DDEs [29]. For the reasons above, in the proposed formulation, the delay is always equal to the time step.

2) Stiffness: Apart from the approximation introduced with the delay, the maximum step $h_{\max}$ is also constrained by the stiffness of the DDAEs and the numerical integration method. In the following, we assume that the system is integrated using the ITM, which is a well-known and widely utilized A-stable integration scheme particularly adequate to handle DAE stiffness.

3) Computational burden: The approach presented in Section IV-A and Section V is based on SSSA, which is valid around an equilibrium. SSSA based techniques in this paper are used to capture a feature of the power system model that is "robust", i.e. does not substantially change by varying the operating point. Hence, the analysis can be carried out only once per network. Some references have addressed a similar problem. For example, see the discussion on the participation matrix and identification of relevant state variables in [23]; and the use of SSSA techniques for non-linear dynamic model reduction in [30].

VI. Case Study

We present simulation results in two power system models. In particular, Section VI-A is based on the IEEE 39-bus New England system and employs the discussions of Sections IV and V for selection of variables and estimation of the maximum admissible time step. Then, Section VI-B considers a 21,177-bus model of the ENTSO-E transmission system. This system is large enough to allow properly discussing the impact of the proposed approach on the convergence and the computational burden of the TDI. All simulations are carried out using the power system analysis tool DOME [31].

A. 39-bus New England System

This section presents simulation results based on the New England 39-bus system, detailed static and dynamic data of which can be found in [32]. It consists of 10 synchronous generators, all represented by 4-th order (two-axis) models [24]; 34 transmission lines; 12 transformers; and 19 loads, which are modeled as constant active and reactive power consumption. Each generator is equipped with AVR, TG and Power System Stabilizer (PSS). and thus provides primary voltage, primary frequency and damping control, respectively, to the system. In this paper, all generators are assumed to participate to secondary frequency and voltage control through AGC and SVR schemes, respectively. Note that the COI speed is used as angular frequency reference of the generators. In total, the system has 141 state variables and 253 algebraic variables.

We apply the variables selection method described in Section IV-A. The state matrix $\boldsymbol{A}$ has 141 finite eigenvalues, 48 of which have natural frequencies that fall in the range $[0.1, 2]$ Hz

TABLE I: New England system: Relative errors of rightmost eigenvalues, $\text{gco}_{\max} = 10^{-10}$.

Delay-free system	$h = 0.01$ s		$h = 0.2$ s		$h = 0.24$ s	
λ_i	$\hat{\lambda}_i$	η_i (%)	$\hat{\lambda}_i$	η_i (%)	$\hat{\lambda}_i$	η_i (%)
-0.00782	-0.00782	0.00	-0.00783	0.13	-0.00784	0.26
$-0.01400 \pm j0.03721$	$-0.01400 \pm j0.03720$	0.03	$-0.01399 \pm j0.03719$	0.06	$-0.01397 \pm j0.03717$	0.13
-0.02000	-0.02000	0.00	-0.02000	0.00	-0.02000	0.00
-0.02890	-0.02890	0.00	-0.02890	0.00	-0.02890	0.00
-0.02998	-0.02998	0.00	-0.02998	0.00	-0.02998	0.00
-0.04009	-0.04009	0.00	-0.04009	0.00	-0.04009	0.00
-0.04368	-0.04368	0.00	-0.04368	0.00	-0.04368	0.00
-0.05554	-0.05554	0.00	-0.05553	0.02	-0.05553	0.02
-0.05776	-0.05776	0.00	-0.05776	0.00	-0.05776	0.00
-0.06160	-0.06160	0.00	-0.06160	0.00	-0.06160	0.00
-0.06179	-0.06179	0.00	-0.06179	0.00	-0.06179	0.00
-0.06312	-0.06312	0.00	-0.06312	0.00	-0.06312	0.00
$-0.08362 \pm j0.02745$	$-0.08364 \pm j0.02748$	0.04	$-0.08388 \pm j0.02770$	0.41	$-0.08426 \pm j0.02804$	0.99
-0.10001	-0.10001	0.00	-0.10001	0.00	-0.10001	0.00
-0.10002	-0.10002	0.00	-0.10002	0.00	-0.10002	0.00

and are thus considered *relevant* eigenvalues for the analysis carried out below. Table II shows the number of non-zero (NNZ) elements of the Jacobian matrix of the original system. The full 394×394 Jacobian matrix $\boldsymbol{A}_c$ has $1,704$ non-zero elements, which corresponds to density 1.098%. The effect of the selected threshold $\text{gco}_{\max}$ on the density of the system Jacobian matrices is shown in Fig. 2. As expected, the higher $\text{gco}_{\max}$, the more elements are selected and the sparser the delayed Jacobian matrices become.

TABLE II: New England system: NNZ Jacobian matrix elements of the original DAE system.

$\boldsymbol{f_x}$	$\boldsymbol{f_y}$	$\boldsymbol{g_x}$	$\boldsymbol{g_y}$	Total	Density (%)
281	271	140	$1,012$	$1,704$	1.098

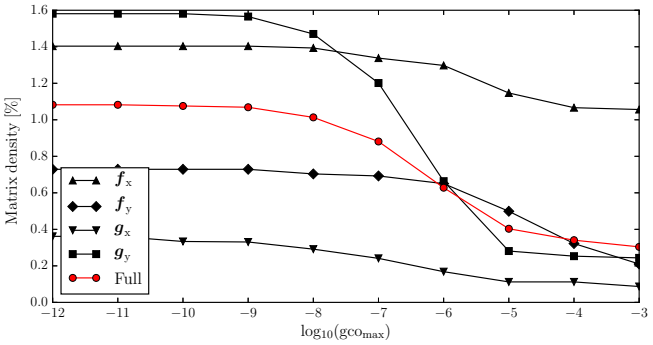

Fig. 2: New England system: Density of Jacobians as $\text{gco}_{\max}$ varies.

For the sake of example, let us consider $\text{gco}_{\max} = 10^{-10}$. In this case, selected variables include variables of TGs; rotor speeds that appear in the equation of the COI; variables of the SVR. The method suggests first variables of slow acting devices, which is also consistent to the discussion of Section IV. The relative errors of the system for the 35 rightmost eigenvalues are calculated according to (26) and results for different delays are presented in Table I. If $h = 0.01$, all relative eigenvalue errors are below 0.05%. The relative eigenvalue errors increase for larger delays. According to the discussion of Section V, if the maximum relative error is $\eta_{\max} = 1\%$, we find $h_{\max} = 0.24$ s. Finally, as illustrated in Fig. 2, constantly increasing $\text{gco}_{\max}$ leads to more and more variables being selected, which gradually limits the value of $h_{\max}$. However, following from (17), variables that inherently define relevant modes are consistently selected.

The geometric approach can always provide an insight in the system structure in a systematic and model-agnostic way, unlike for example, the methods proposed in [20] and [21]. This feature is particularly important for modern power systems where converter-interfaced devices can change, in a future not too far away, the overall dynamic response of the system. Still, it is common that variables of a conventional power system DAE model are well-known. Then, $\boldsymbol{x}_d$, $\boldsymbol{y}_d$ can be selected based on the user's experience, and thus without applying a systematic method. The variables that if delayed, do not change or change in a negligible way the overall dynamic behavior of the system, are typically the ones with significantly slower dynamic response as compared to the critical modes of the system. Selected variables are thus naturally decoupled by the critical dynamics of the system due to their different time scale. With this regard, we have two comments. First, for any set of selected elements, $h_{\max}$ is not known a priori, so it can be still estimated according to the method described in Section V. Second, while selecting $\boldsymbol{x}_d$, $\boldsymbol{y}_d$, the user should take into account that, how slow a variable actually is depends on the state matrix $\boldsymbol{A}$ and, in turn, on the parameters of the examined system. For example, consider again the example of the COI. Differentiation of (18) yields:

$$\dot{\omega}_{\text{COI}} = \sum_{i=1}^{\kappa} \frac{M_i}{M_T} \dot{\omega}_i \ , \tag{28}$$

where $\dot{\omega}_i$ is given by the well-known swing equation:

$$\dot{\omega}_i = \frac{1}{M_i}(\tau_{\text{m},i} - \tau_{\text{e},i} - D_i(\omega_i - \omega_{\text{COI}})) \ , \tag{29}$$

where $\tau_{\text{m},i}$, $\tau_{\text{e},i}$ are the mechanical and electrical torque, respectively; D_i is the damping coefficient of the i-th machine.

Substitution of (29) to (28) gives:

$$\dot{\omega}_{\mathrm{COI}} = \frac{1}{M_T}\left(\tau_{\mathrm{m},T} - \tau_{\mathrm{e},T} - \sum_{i=1}^{\kappa} D_i(\omega_i - \omega_{\mathrm{COI}})\right) , \quad (30)$$

where $\tau_{\mathrm{m},T} = \tau_{\mathrm{m},1} + \tau_{\mathrm{m},2} + \ldots + \tau_{\mathrm{m},\kappa}$; and $\tau_{\mathrm{e},T} = \tau_{\mathrm{e},1} + \tau_{\mathrm{e},2} + \ldots + \tau_{\mathrm{e},\kappa}$. A characteristic of the 39-bus system is that $M_1 \gg M_i$, $i \neq 1$ ($M_1 = 1000$ MWs/MVA, while the second larger mechanical starting time is $M_{10} = 84$ MWs/MVA). In this case, the rate of change of ω_{COI} is still slow (see Section IV-B), but as seen from (30) its rate of change is comparable with that of ω_1.

As it can be observed, delayed variables are associated with secondary controllers or "slow" variables such as the center of inertia. The dynamic response of such variables cannot change even for relatively big changes of the operating point and topology of the system. As a matter of fact, one could select *a priori* most of these variables. However, the eigenvalue analysis

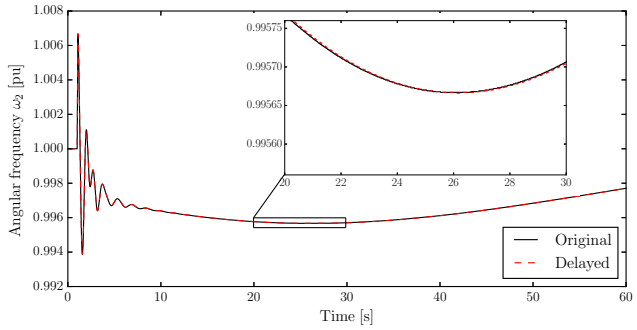

(a) $h = 0.02$ s.

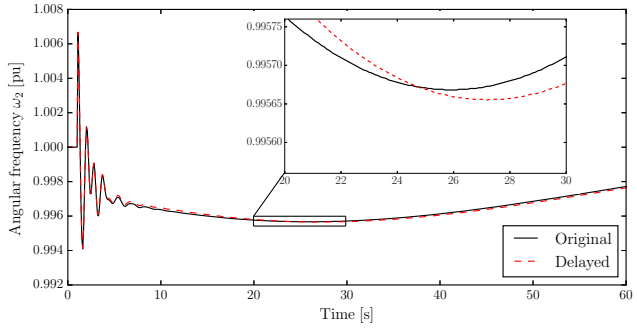

(b) $h = 0.10$ s.

Fig. 3: New England system: Transient following a three-phase fault.

We provide an example on the effect of the one-step delay approximation in the transient response of the 39-bus system by carrying non-linear time domain simulations. With this aim and according to the discussion of Section IV-B, we eliminate the dense segments $\partial g_{(\omega_{\mathrm{COI}})}/\partial \omega_i$, $\partial f_{(\dot{\delta}_i)}/\partial \omega_{\mathrm{COI}}$, $\partial g_{(p_{\mathrm{ord},i})}/\partial p_{\mathrm{s}}$, $\partial f_{(x_{r,i})}/\partial \boldsymbol{q}_{\mathrm{r}}$, that arise from (18)-(21). We simulate the transient following a three-phase fault applied at bus 6 at $t = 1$ s. The fault is cleared after 80 ms by tripping the transmission line that connects buses 5 and 6. The system is numerically integrated using the ITM. Figure 3 shows the transient behavior of the rotor speed of generator 2 for integration step sizes $h = 0.02$ s and $h = 0.1$ s. As it can be seen, the larger h is, the larger is the mismatch between the two trajectories. In both plots though, the trajectory of the DDAE system closely follows the original trajectory, as expected.

We check the accuracy of the proposed one-step delay technique under different operating conditions and contingencies. In addition to the operating condition considered above (from here and on referred as the base case), we consider two more operating conditions, namely, 10% and 20% increase in the total power consumption of the system. For each operating point, we examine the transient response of the system. We consider two different disturbances: first, the three phase fault applied at bus 6 described above; and second, the loss of the load connected at bus 39 at $t = 1$ s, which leads to a 1.109 GW decrease in the power consumption of the system. In all scenarios, the delayed variables do not change and are the ones used to plot the base case in Fig. 3.

The response of the rotor speeds of the DAE system are compared with the respective speed trajectories obtained by integrating the DDAE system. Each system is simulated for 100 s and for two time step sizes, $h = 0.02$ s and $h = 0.10$ s. The maximum absolute rotor speed trajectory errors are summarized in Table III. As expected, the proposed technique shows high accuracy for all considered operating conditions and disturbances.

TABLE III: New England system: Maximum absolute rotor speed trajectory mismatches induced by the proposed method.

Operating condition	Applied disturbance	$h = 0.02$ s – max. error	$h = 0.10$ s – max. error
Base case	Fault at bus 6	$6.0 \cdot 10^{-6}$	$8.3 \cdot 10^{-5}$
	Bus 39 load trip	$9.0 \cdot 10^{-6}$	$4.2 \cdot 10^{-5}$
+10% load	Fault at bus 6	$6.0 \cdot 10^{-6}$	$4.8 \cdot 10^{-4}$
	Bus 39 load trip	$1.2 \cdot 10^{-5}$	$5.7 \cdot 10^{-5}$
+20% load	Fault at bus 6	$7.0 \cdot 10^{-6}$	$5.8 \cdot 10^{-4}$
	Bus 39 load trip	$1.7 \cdot 10^{-5}$	$8.4 \cdot 10^{-5}$

B. 21,177-bus ENTSO-E System

This subsection presents simulation results on a dynamic model of the ENTSO-E transmission system. The system includes 21,177 buses (1,212 off-line); 30,968 transmission lines and transformers (2,352 off-line); 1,144 zero-impedance connections (420 off-line); 4,828 power plants represented by 6-th order and 2-nd order synchronous machine models; and 15,756 loads (364 off-line), modeled as constant active and reactive power consumption. Synchronous machines represented by 6-th order models are also equipped with dynamic AVR and TG models. Moreover, the system includes 364 PSSs. Finally, the system includes AGC and SVR mechanisms, which provide secondary frequency and voltage control, respectively, to different areas of the system. In total, the system has 49,930 state variables and 97,304 algebraic variables. The full Jacobian matrix has dimensions $147,234 \times 147,234$ and

$1,226,492$ non-zero elements, which yields a density degree of 0.0057 %.

We show the impact of the one-step delay approximation on the accuracy, number of factorizations and computational burden of the TDI. To this aim, the dense segments that arise from (18)-(21) are eliminated, leading to a sparser and less coupled model. The NNZ Jacobian elements of the original and delayed system are summarized in Table IV.

TABLE IV: ENTSO-E system: NNZ Jacobian elements.

System	NNZ Jacobian elements	Density (%)	Relative diff.
Original	$1,226,492$	0.0057	
Delayed	$936,871$	0.0043	-23.61 %

We consider a three-phase fault at bus $12,921$, occuring at $t = 1$ s. The fault is cleared after 100 ms. The response of the rotor speed of the synchronous generator connected at bus $2,292$ during the first seconds following the fault, is shown in Fig. 4 for two different time step sizes. As it can be

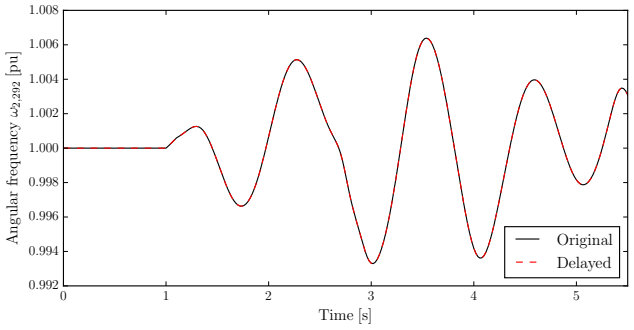

(a) $h = 0.02$ s.

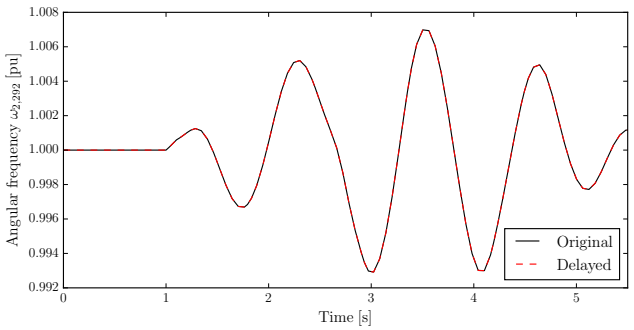

(b) $h = 0.06$ s.

Fig. 4: ENTSO-E system: Transient following a three-phase fault.

seen, the difference between the two trajectories is very small, which indicates that accuracy is maintained. In particular, the maximum absolute mismatch between the two trajectories for the cases shown in Fig. 4 are: (a) $1.0 \cdot 10^{-6}$, (b) $7.0 \cdot 10^{-6}$.

We examine the impact of the one-step delay approximation on the number of factorizations of the TDI. Following a disturbance, the system shows a transient and, provided that the trajectory is stable, finally reaches a stationary point. While in steady state, the ITM requires exactly one factorization for each time step, both for the original and the delayed system. Hence, any noticeable differences in the number of factorizations required by the original and the delayed system occur during the first seconds following the disturbance.

The number of factorizations required by the original and the delayed system during the first seconds following the three-phase fault, are shown in Fig. 5. Since the increments of the variables at each time step are updated according to the standard Newton method (see Section II), the number of factorizations at each time step is equal to the number of Newton iterations. As it can be seen, the original and the delayed system in this case require the same number of factorizations at each time step to converge, which indicates that the approximation does not jeopardize the convergence.

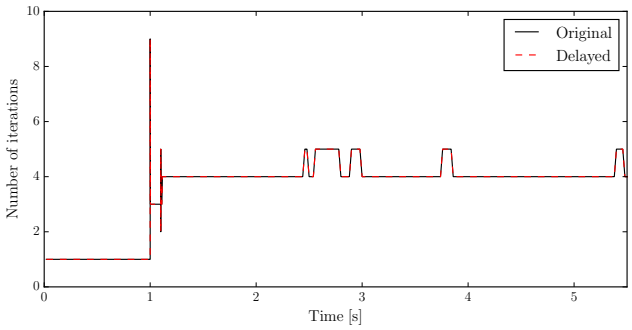

(a) $h = 0.02$ s.

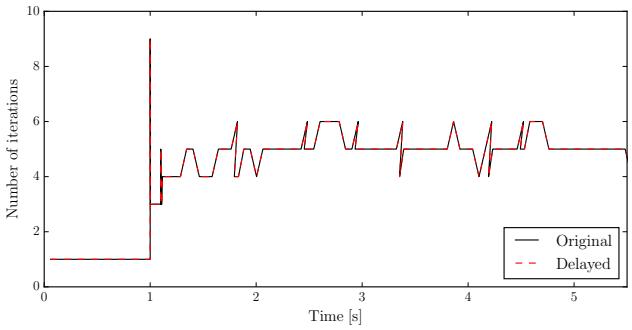

(b) $h = 0.06$ s.

Fig. 5: ENTSO-E system: Number of Newton iterations.

We finally discuss the effect of the one-step delay approximation on the computational burden of the TDI. The method reduces the coupling of the ENTSO-E system and facilitates the potential application of techniques that factorize decoupled blocks of the Jacobian matrix in parallel. In turn, enabling parallelization leads to a significant speedup of the simulation. However, as already discussed, the goal of this paper is to provide a technique for decoupling and sparsity increase rather than applying parallel techniques. Hence, we provide a comparison of the original and delayed ENTSO-E system in terms of computational effort required for a non-parallel numerical integration.

The full Jacobian matrix without introducing delays requires 0.245 s per single factorization, in average, on a $8\times$ 3.5 GHz Intel Xeon CPU desktop computer, while the Jacobian matrix of the delayed system requires 0.223 s, which corresponds to a speedup of 9.04 %.

Apart from the factorization speed-up, one has also to evaluate whether the delayed system requires more or less iterations than the original system to solve the Newton method for each point of the time domain integration. With this regard, we have already shown an example in Fig. 5, where the two systems require at each point the same number of iterations. In addition, we have carried out several cases considering a variety of contingencies and time steps and found out that the proposed technique is able to reduce the simulation time in range from 5 to 20%.

For the sake of example, consider the three-phase fault at bus $2,292$ discussed above. The system is integrated for 7 s. With a time step $h = 0.02$ s, the original system completes the numerical factorization in 298.63 s, while the delayed system in 262.14 s, which corresponds to a speedup of 12.22 %.

The proposed one-step-delay technique is agnostic with respect to the integration scheme utilized for the TDI. For this reason, the proposed approach can be coupled with any other numerical technique to speed up time domain simulation software. Hence, even if the speed-up provided by the proposed formulation *per se* is not huge, such a speed-up can be combined with that of other techniques. Moreover, reducing the computational burden is not the only benefit of the proposed one-step delay technique. A relevant feature is that it increases the decoupling of system variables. This leads to a sparser and more decoupled system Jacobian matrix. The latter is a feature that we expect to be beneficial to further speed up the time domain analysis if combined with parallelization techniques.

VII. Conclusions

The paper proposes a systematic approach to exploit delays to reduce the coupling of the equations of conventional DAE models of power systems for transient stability analysis. With this aim, the paper discusses how to select the elements of a power system DAE model that can be delayed and provides an estimation of the maximum admissible time delay so that simulation accuracy is maintained. Numerical simulations provide a first, simplified evaluation of the proposed approach, in terms of accuracy, convergence and computational burden. Future work will focus on potential applications such as embedding the proposed approach in algorithms that apply state-of-the art parallelization techniques.

References

[1] A. Bellen, N. Guglielmi, and A. E. Ruehli, "Methods for linear systems of circuit delay differential equations of neutral type," *IEEE Trans. Circ. Syst. I*, vol. 46, no. 1, pp. 212–215, Jan. 1999.

[2] R. A. Minasian, "Photonic signal processing of microwave signals," *IEEE Trans. Microwave Theory and Techniques*, vol. 54, no. 2, pp. 832–846, Feb. 2006.

[3] V. Venkatasubramanian, H. Schattler, and J. Zaborszky, "A time-delay differential-algebraic phasor formulation of the large power system dynamics," in *ISCAS*, vol. 6, May 1994, pp. 49–52.

[4] J. W. Stahlhut, T. J. Browne, G. T. Heydt, and V. Vittal, "Latency viewed as a stochastic process and its impact on wide area power system control signals," *IEEE Trans. Power Syst.*, vol. 23, no. 1, pp. 84–91, Feb. 2008.

[5] M. Liu, I. Dassios, G. Tzounas, and F. Milano, "Stability analysis of power systems with inclusion of realistic-modeling WAMS delays," *IEEE Trans. Power Syst.*, vol. 34, no. 1, pp. 627–636, Jan. 2019.

[6] K. S. Ko and D. K. Sung, "The effect of EV aggregators with time-varying delays on the stability of a load frequency control system," *IEEE Trans. Power Syst.*, vol. 33, no. 1, pp. 669–680, Jan. 2018.

[7] Á. Ortega and F. Milano, "Comparison of different PLL implementations for frequency estimation and control," in *ICHQP*, May 2018.

[8] N. Watson and J. Arrillaga, *Power systems electromagnetic transients simulation*. London, UK: The IET, 2003.

[9] J. Mahseredjian, L. Dube, Ming Zou, S. Dennetiere, and G. Joos, "Simultaneous solution of control system equations in EMTP," *IEEE Trans. Power Syst.*, vol. 21, no. 1, pp. 117–124, Feb 2006.

[10] F. M. Uriarte, *Multicore Simulation of Power System Transients*. London, UK: The IET, 2013.

[11] L. L. Grigsby, *Power System Stability and Control*. Boca Raton, CA: CRC Press, 2007.

[12] M. Shahidehpour and Y. Wang, *Communication and Control in Electric Power Systems*. Hoboken, NJ: John Wiley & Sons, 2003.

[13] G. Kron, *The piecewise solution of large-scale systems*. London, UK: Macdonald, 1963.

[14] F. M. Uriarte, "On Kron's diakoptics," *Electric Power Syst. Research*, vol. 88, pp. 146 – 150, 2012.

[15] I. Kocar, J. Mahseredjian, U. Karaagac, G. Soykan, and O. Saad, "Multiphase load-flow solution for large-scale distribution systems using mana," *IEEE Trans. Power Deliv.*, vol. 29, no. 2, pp. 908–915, Apr. 2014.

[16] U. Karaagac, J. Mahseredjian, I. Kocar, G. Soykan, and O. Saad, "Partial refactorization based machine modeling techniques for electromagnetic transients," in *IEEE PES General Meeting*, Jul. 2017.

[17] D. Fabozzi and T. V. Cutsem, "On angle references in long-term time-domain simulations," *IEEE Trans. Power Syst.*, vol. 26, no. 1, pp. 483–484, Feb. 2011.

[18] B. Stott, "Power system dynamic response calculations," *Procs of the IEEE*, vol. 67, no. 2, pp. 219–241, Feb. 1979.

[19] F. Milano and M. Anghel, "Impact of time delays on power system stability," *IEEE Trans. Circ. Syst. I*, vol. 59, no. 4, pp. 889–900, Apr. 2012.

[20] J. Fong and C. Pottle, "Parallel processing of power system analysis problems via simple parallel microcomputer structures," *IEEE Trans. Power App. Syst.*, vol. PAS-97, no. 5, pp. 1834–1841, Sep. 1978.

[21] D. Fabozzi, A. S. Chieh, B. Haut, and T. V. Cutsem, "Accelerated and localized Newton schemes for faster dynamic simulation of large power systems," *IEEE Trans. Power Syst.*, vol. 28, no. 4, pp. 4936–4947, Nov. 2013.

[22] H. Hamdan and A. Hamdan, "On the coupling measures between modes and state variables and subsynchronous resonance," *Elec. Power Syst. Res*, vol. 13, no. 3, pp. 165 – 171, 1987.

[23] G. C. Verghese, I. J. Pérez-Arriaga, and F. C. Schweppe, "Selective modal analysis with applications to electric power systems, part ii: The dynamic stability problem," *IEEE Power Eng. Rev.*, vol. PER-2, no. 9, pp. 30–31, Sep. 1982.

[24] F. Milano, *Power System Modelling and Scripting*. London, UK: Springer, 2010.

[25] C. W. Taylor and R. L. Cresap, "Real-time power system simulation for automatic generation control," *IEEE Trans. Power App. Syst.*, vol. 95, no. 1, pp. 375–384, Jan 1976.

[26] G. Sulligoi, M. Chiandone, and V. Arcidiacono, "New SART automatic voltage and reactive power regulator for secondary voltage regulation: Design and application," in *IEEE PES General Meeting*, Jul. 2011.

[27] F. Milano and I. Dassios, "Small-signal stability analysis for non-index 1 Hessenberg form systems of delay differential-algebraic equations," *IEEE Trans. Circ. Syst. I*, vol. 63, no. 9, pp. 1521–1530, Sep. 2016.

[28] W. Michiels and S.-I. Niculescu, *Stability and Stabilization of Time-Delay Systems: An Eigenvalue-Based Approach*. Philadelphia, PA: SIAM, 2009.

[29] N. Guglielmi and E. Hairer, "Implementing Radau IIA methods for stiff delay differential equations," *Computing*, vol. 67, no. 1, pp. 1–12, Jul. 2001.

[30] J. H. Chow, *Power system coherency and model reduction*, ser. Power Electronics and Power Systems 94. New York: Springer-Verlag, 2013.

[31] F. Milano, "A Python-based software tool for power system analysis," in *IEEE PES General Meeting*, Jul. 2013.

[32] F. Milano and Á. Ortega Manjavacas, *Converter-Interfaced Energy Storage Systems: Context, Modelling and Dynamic Analysis*. Cambridge University Press, 2019.

Georgios Tzounas (S'17) received from National Technical University of Athens, Greece, the ME in Electrical and Computer Engineering in 2017. Since September 2017, he is Ph.D. candidate with Univ. College Dublin, Ireland. His scholarship is funded through the SFI Investigator Award with title "Advanced Modeling for Power System Analysis and Simulation" (AMPSAS). His current research interests include stability analysis and robust control of power systems.

Federico Milano (F'16) received from the Univ. of Genoa, Italy, the ME and Ph.D. in Electrical Eng. in 1999 and 2003, respectively. From 2001 to 2002 he was with the Univ. of Waterloo, Canada, as a Visiting Scholar. From 2003 to 2013, he was with the Univ. of Castilla-La Mancha, Spain. In 2013, he joined the Univ. College Dublin, Ireland, where he is currently Prof. of Power Systems Control and Protections and Head of Elec. Eng. His research interests include power system modeling, control and stability analysis.